Dynamical Lifetimes of Objects Injected into Asteroid Belt Resonances

Brett J. Gladman,* Fabbio Migliorini, Alessandro Morbidelli, Vincenzo Zappalà, Patrick Michel, Alberto Cellino, Christiane Froeschlé, Harold F. Levison, Mark Bailey, Martin Duncan

Numerical simulations of particles placed in orbital resonances in the main asteroid belt show that the typical dynamical lifetimes of objects that could become near-Earth asteroids or meteorites are only a few million years, with the majority destroyed by being transferred to Jupiter-crossing orbits or being driven into the sun. Particles that fortuitously migrate to the terrestrial planet region may be pushed to high-inclination orbits by resonances but are still dynamically eliminated on time scales of ~10 million years. These shorter lifetimes may require a reassessment of our qualitative understanding about near-Earth asteroids and meteorite delivery.

The main asteroid belt is considered to be the source of most meteorites and probably the majority of near-Earth asteroids (NEAs). Our understanding of the mechanisms that transport objects from the main belt to Earth has evolved over the past three decades. We have moved from the idea that it was difficult, if not impossible, to remove objects from the belt, to an understanding that resonant phenomena can increase eccentricities to the point where Earth collisions are possible (*1*). This progress is due to advances in analytical modeling of resonant phenomena and the use of numerical experiments as computational power has increased.

Analytic theories of the dynamics in the main belt (*2*) indicate that many secular and mean-motion resonances are capable of transporting particles to Mars-crossing, and often Earth-crossing, orbits. The gravitational attraction of a planet can then pull these particles out of the resonances, and subsequent close encounters modify the orbits of the extracted particles. A qualitative understanding has emerged (*3*) that the resonant phenomena tend to operate quickly and result in orbits that become either sun-grazing (*4*) or Jupiter-crossing. Particles that escape the resonances by means of planetary close encounters wander more slowly until they find a strong resonant region in which their dynamical lifetimes are short, unless they fortunately escape by another extraction event. This general picture was illustrated with numerical integrations for time scales on the order of a few million years (*3*), but because the particles chosen for the integrations were the most potentially unstable ones, it was unclear how generic the effects might be for particles deep inside the main belt. To address this question, we numerically integrated ≃1500 particles initially placed in the most important main-belt resonances.

B. J. Gladman, A. Morbidelli, P. Michel, Ch. Froeschlé, Observatoire de la Côte d'Azur, Boite Postale 4229, 06304 Nice Cedex 4, France. F. Migliorini and M. Bailey, Armagh Observatory, College Hill BT61 9DG, Northern Ireland, UK. V. Zappalà and A. Cellino, Osservatorio Astronomico di Torino, I-10025 Italy. H. F. Levison, Southwest Research Institute, Boulder, CO 80302, USA. M. Duncan, Department of Astronomy, Queen's University, Ontario K7L 3N6, Canada.

*To whom correspondence should be addressed. E-mail: gladman@obs-nice.fr

Initial Conditions and Method

The original intent of this project, known as GAPTEC (*5*), was to dynamically associate NEAs of known taxonomic type with asteroid families near main-belt resonances with Jupiter. Examining proper orbital elements of the family members and the location of the borders of neighboring resonances (*6*) shows that some asteroid families are truncated by a resonance. This implies that the family-creation event injected kilometer-scale fragments (now gone) into the resonance. To estimate their original distribution, we calculated ejection velocities of known family members in the reference frame of the family's parent body (*7*). For some families (Table 1) the ejection velocity fields have a discontinuity coinciding with the borders of the nearby resonance. The velocity fields were extrapolated, and the region of overlap with the resonance was determined. We then randomly generated 150 particles inside the overlapping region; the initial locations in the ejection-velocity space of these particles were transformed into orbital-element space (Fig. 1) using Gauss' equations (*7*).

This procedure had two exceptions: the Koronis (K) family and the Vesta family (V). The K family exhibits a complex structure (*8*), with the presence of a possible secondary event forming a "tail" of fragments located toward the edge of the 7:3 (Fig. 1). The structure of the ejection velocity field for this secondary event cannot be reliably reconstructed; thus, the simulated fragments injected into the 7:3 resonance were chosen by visual inspection of the proper elements of the known family members. The choice of initial conditions for V objects emplaced in the 3:1 and ν_6 resonances is discussed in (*9*).

In addition to the 150 particles injected into the neighboring resonances for each family, we also generated 15 particles close to the resonance border but not inside the zone of libration. These particles might diffuse (*8, 10*) into the resonance on some unknown time scale.

The details of these initial conditions are not important, because we are interested in studying the dynamical time scales associated with the resonances. Although these initial conditions (Fig. 1) were chosen in the context of family-generated fragments, they also provide a reasonable sample of initial conditions for injected particles that might deliver meteorites to Earth. The 3:1 and 5:2 resonances were each well sampled at three eccentricity (e) and inclination (i) regions. In particular, there was no bias toward the most unstable portions of the resonances. This must be qualified for the case of the ν_6, where the initial conditions are very deep inside the resonance, and thus the time scales we find are biased toward quick deliveries to Earth-crossing orbits; this simulation must be viewed as exploring how objects that reach this portion of the resonance evolve.

The integration was accomplished with a mixed-variable symplectic algorithm adapted to resolve planetary close encounters. Comparisons with other integrators yielded consistent results over time scales of a few million years (*11*). Orbital histories were followed for up to ~100 My, terminating if the particles struck a planet or the sun or were found exterior to Saturn's orbit (in which case they will be removed from the solar system on time scales of 10^4 to 10^5 years). Simulations also terminated if no "active" particles remained (except for the 7:3 and 8:3 simulations, which were stopped because of computational length). Active particles are those for which an examination of the resonant argument indicates some interaction with the resonance.

End States and Time Scales

Because the resonance boundaries are imperfectly located, not all the particles were in the resonance during the simulation (*12*); thus, the statistics are based on only the active particles (Table 1). By far the dominant end states are solar impact and having orbital aphelion (Q) past Saturn. Solar impacts dominate for initial semimajor axes $a < 2.5$ AU. Particles initially outside $a = 2.5$ AU are perturbed toward $e \simeq 1$, causing them to cross Jupiter's orbit and be removed. Poisson statistics govern the rare planetary impacts (Table 1); the higher incidence for the case of the ν_6 resonance is statistically valid. We tabulated the time required for 50 and 90% of the active particles to die, as well as the median time T_{cr} required for particles to cross the orbits of Mars, Earth, and Venus; for example, T_{cr} Earth is the median time for objects to reach perihelion $q < a(1 - e) = 1$ AU, based on the subset that ever satisfy this condition. The 90% decay time is based on ~10 particles and is thus less well determined than the half-life.

The agreement in terms of end states and half-lives for the different samples of particles injected into the 3:1 and 5:2 is striking, confirming that these resonances are almost globally chaotic (*13*). Long-term dynamical behavior in these resonances is, to a first approximation, independent of the injection location. The decay of the number of particles with time (Fig. 2) in these cases is so similar that we plot only one sample decay curve for each. We have strengthened this assertion by integrating another 987 particles at $i = 10°$, uniformly filling the 3:1 between $e = 0$ and 0.3; again, the decay curve is statistically identical to that of Fig. 1. The universality of time scale does not hold for the ν_6 because the central portion of the resonance we sampled is one of the strongest and thus is probably not typical for injected fragments, most of which will require more time to reach Earth-crossing orbits.

The median lifetimes are roughly one order of magnitude lower than those usually discussed that are based on Öpik-type evolution models (*14, 15*). This discrepancy can be attributed to the importance of sun-grazing dynamics (*3, 4*) and the existence of secular resonances inside main-belt mean-motion resonances (*13*). The 3:1 and ν_6 resonances are powerful and capable of pumping e to 1 on million-year time scales. These resonances efficiently annihilate the NEA population with $a > 2$ AU, and do not just deliver them to Earth-crossing orbits.

All the resonances exhibit diffusive tails; that is, particles not in the resonance can slowly diffuse in phase space until they encounter a strong region (*8, 10*). They are then destroyed on the characteristic time scale of the resonance. This process produces the tail of long-lived objects exhibited by the 5:2 (Fig. 2); these particles do not exit the main belt and then live for a long time, but rather spend tens of millions of years diffusing in or near the resonance and then die on the ~0.5-My characteristic time of the resonance. For the 3:1 some of the tail, and for the ν_6 almost all of the tail, is instead due to particles that migrate to long-living orbits at $a < 2$. The half-life estimates are relatively unaffected by the diffusive particles because median half-lives are used.

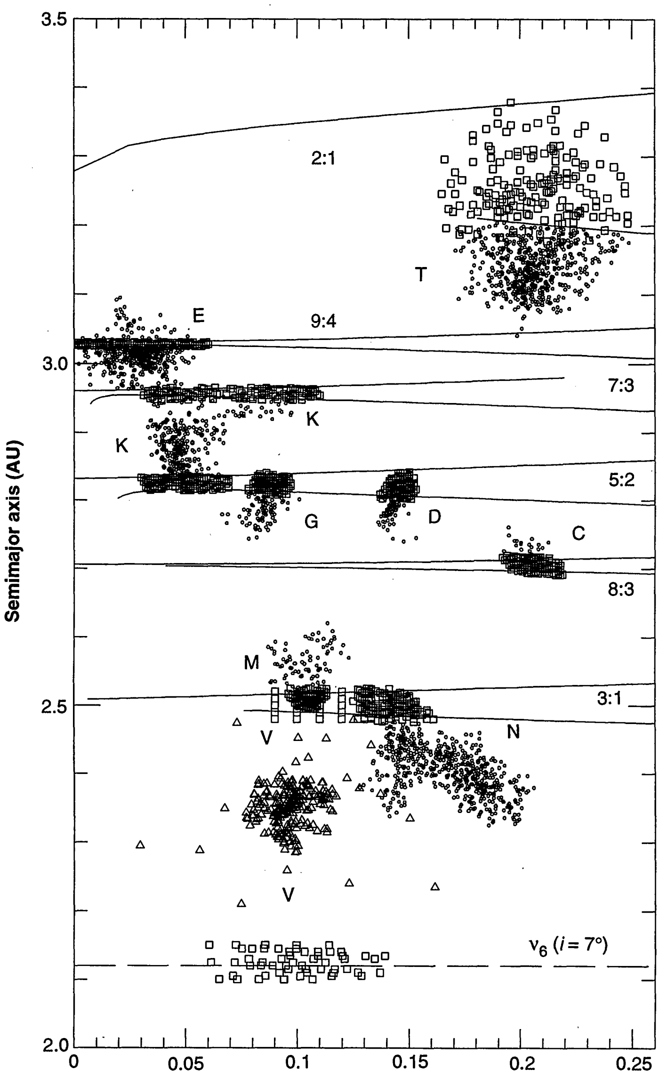

Fig. 1. Resonant proper elements for the integrated particles and the "parent" asteroid families. Family members [small circles (except Vesta family members, which are triangles)] are labeled by the first letter of the family name (Table 1). Particles (squares) injected into the nearby resonance are unambiguously associated with each parent family, except for the 3:1 Vesta injections, which lie on a grid partly overlapping the Maria and Nysa injections. Approximate resonance boundaries are shown, as well as the center of the ν_6 resonance (which does not have a width in the usual sense) for the median inclination ($i = 7°$) of the Vesta fragments. The resonances correspond to the Kirkwood gaps in the asteroid distribution (*34*).

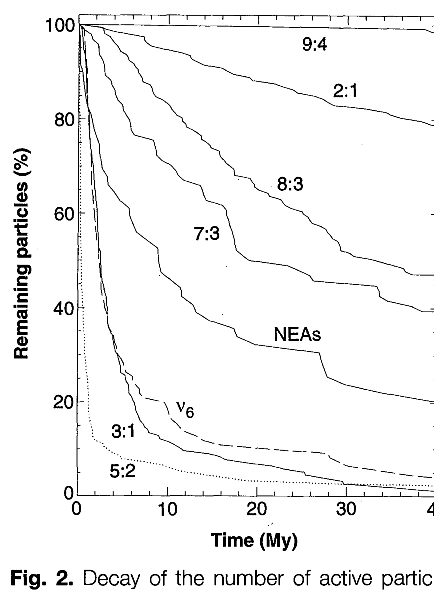

Fig. 2. Decay of the number of active particles versus time. The ν_6, 3:1, and 5:2 resonances are characterized by very short lifetimes for most resonant particles, with long diffusive tails. The outer resonances studied (7:3, 9:4, and 2:1) also have short lifetimes after the particle finds the strong portion of the resonance, but finding these strong regions typically requires tens of millions of years. The NEA decay curve is shown for comparison; this figure should not be taken to indicate any particular resonance as their source.

Evolutionary Paths

Typical evolutionary paths (Fig. 3A) from the ν_6, 3:1, and 5:2 resonances involve particles being pushed into sun-grazing or Jupiter-crossing orbits on million-year time scales. After reaching planet-crossing e's, close encounters with the inner planets can extract particles from the resonance. Because of necessarily limited numerical output, it is often impossible to tell from our integrations whether extraction close-encounters were with Earth or Venus, so we combined them (Table 1). For mean-motion resonances outside 2.5 AU, such a close encounter breaks the inherent phase-protection of the resonance (*16*), permitting Jupiter encounters that subsequently remove the particle from the inner solar system. The 3:1 is borderline in this regard; it is so strong that it often pushes particles into the sun (Fig. 3A) before close encounters extract them and allow approaches to Jupiter. The ν_6 is less effective at pushing particles directly into the sun than the 3:1 (Table 1); usually the particle is extracted for a brief period before reentering and being pushed into the sun by the ν_6 or 3:1 (Fig. 3A). Most extracted 3:1 particles reenter that resonance or the ν_6 and then hit the sun. The final stage of sun-grazing is dynamically complex (*4*).

Thus, Earth-crossing orbits with $a > 2$ are rapidly (10^5 to 10^6 years) produced from resonant injections; however, once placed in the Apollo or Amor regime (*17*), the residence time is also short. Objects rarely migrate down to smaller a through close encounters; we compiled statistics of those particles that ever (however briefly) have $a < 2$ AU, $a < 1$ AU, or aphelia $Q < 2$ AU, as well as the median duration in that state (Table 1). Although in some cases the small number of particles that enter these states results in poorly determined time scales, we claim that the majority of bodies that enter the NEA population do so transiently; most come below $a = 2$ AU only for a brief residence of ~1 My and then return to $a > 2$ AU to be pushed into the sun by the ν_6 or 3:1 resonance. The current NEA population will be biased toward the longest living objects because they are more likely to survive and be observed; we integrated a sample of 178 real NEAs and found a median half-life (Fig. 2) of ~10 My; simulated particles that migrate into the inner solar system show similar half-lives.

An example from the ν_6 (Fig. 3B) is instructive, although exceptionally long-lived. Resonant e oscillations initially produce only a Mars-crossing orbit; small changes in a caused by repeated Mars encounters move the orbit in the resonant phase space until after 4 My it finds the powerful portion of the resonance that quickly makes it cross the orbit of Earth. It visits quasi-stable regions near $a = 1.5$ and 1.65 AU (in that order) before wandering down into the terrestrial region—which includes two excursions to $e < 0.1$, the first being an SEA-like (*18*) nearly circular orbit barely interior to Earth—after 20 My. It then returns to the main belt and is pushed into the sun by the ν_6 resonance at $t = 30$ My. During its lifetime, this particle is influenced by the ν_5, ν_6, ν_{16}, ν_2, ν_3, ν_4, and $2g = g_5 + g_6$ secular resonances, with the latter three being dominant during the 7-My period trapped near 1.5 and ≃1.6 AU (*19*, *20*); in fact, some resonant phenomenon is almost constantly operating and the particle is just handed from one resonance to the next. An example from the 3:1 (Fig. 3C) shows resonant phenomena in the horizontal oscillations that occur when reso-

Table 1. Summary of the numerical simulations. Resonant injections are labeled by the asteroid family, and the fraction of particles suffering each fate or surviving the entire integration is given. Time scales are shown for 50% (half-life) and 90% decay of the active particles, and median times T_{cr} for crossing the orbits of Mars, Earth, and Venus. We list the percentage of particles that undergo extraction by Mars or by Earth and Venus combined (E/V), go directly into the sun before an extraction event, or acquire certain orbits, with the median time spent in those orbits (T_{med}). Dashes indicate no simulated particles evolved in that way. The semimajor axis a_{res} of the center of the ν_6 resonance depends on the inclination: $a_{res} \simeq 2.1$ astronomical units (AU) for $i = 7°$. The evolution statistics for the 8:3 resonance are based on only the first 29 million years (My) of the simulation. Q indicates orbital aphelion.

	Vesta		Nysa	Maria	Chloris	Dora	Gefion	Koronis		Eos	Themis
	ν_6	3:1	3:1	3:1	8:3	5:2	5:2	5:2	7:3	9:4	2:1
a_{res} (AU)	≃2.1	2.50	2.50	2.50	2.71	2.82	2.82	2.82	2.96	3.03	3.28
Mean initial i (degrees)	7	6	3	15	10	8	9	2	2	9	1
Length (My)	100	18	100	61	42	100	100	17	40	120	100
Active particles (n)	110	92	145	156	157	152	146	84	94	134	153
					End states (%)						
Impact sun	79.1	75.0	69.7	69.8	17.2	7.9	7.5	6.0	0	2.2	6.5
Impact Venus	1.8	0	0	0.6	0	0	0	0	0	0	0
Impact Earth	5.5	0	0.7	0	0	0	0	1.2	0	0	0
Impact Jupiter	0	0	0.7	0.6	0	0	0	4.8	1.1	0	0.7
Outside Saturn	11.8	25.0	28.3	28.8	35.7	92.1	92.5	88.1	56.6	25.4	22.9
Survivors	1.8	0	0.7	0	47.1	0	0	0	42.3	72.4	69.9
					Time scales (My)						
Half-life	2.3	2.1	2.6	2.5	34.0	0.4	0.6	0.7	19.0	>120	>100
90% decay	21.0	6.4	7.3	11.4	>42	3.4	2.9	3.8	>40	>120	>100
T_{cr} Mars	0.24	0.20	1.0	0.32	10.1	0.02	0.13	0.28	10.0	79.5	22.5
T_{cr} Earth	0.50	1.1	1.4	0.96	11.0	0.22	0.41	0.63	6.3	90.0	27.8
T_{cr} Venus	0.70	1.3	1.9	1.2	13.0	0.31	0.45	0.67	2.2	87.9	31.6
					Evolution (%)						
Extracted by Mars	8.2	3.3	5.5	4.5	16.6	–	0.7	–	42.6	30.5	3.3
Extracted by E/V	87.3	66.3	66.2	70.5	32.5	99.3	99.3	100	4.3	0.7	21.6
Direct to sun	4.5	30.4	28.3	25.0	–	0.7	–	–	–	–	3.3
Ever have $a < 2$ AU	53.6	8.7	9.0	7.7	0.6	0.7	1.4	3.6	–	0.7	–
T_{med} (My)	1.5	0.27	0.5	1.4	2.9	39.0	0.6	0.1	–	5.8	–
Ever have $a < 1$ AU	9.1	–	0.7	0.6	–	–	–	–	–	–	–
T_{med} (My)	2.8	–	0.04	13	–	–	–	–	–	–	–
Ever have $Q < 2$ AU	12.7	–	2.1	1.3	–	0.7	–	–	–	0.7	–
T_{med} (My)	6.3	–	0.2	13	–	2.0	–	–	–	4.1	–

nances modify e at constant a; this particle travels back out to the 3:1 and then into the sun after a long lifetime of 26 My.

Each resonance has individual qualities. The ν_6 is wide and is centered at different a for each i (2). The 3:1 is extremely efficient at pushing particles to $e = 1$. Dynamics near Chloris are complicated by interaction with the nearby $g = 2g_6 - g_5$ secular resonance, which serves as an additional source of diffusion (21). The 5:2 increases to $e \simeq 0.8$ in only a few hundred thousand years. Only small portions of the 7:3 are strong, so objects wander for $\sim 10^7$ years before finding a region that pushes them rapidly ($<10^6$ years) to Jupiter-crossing orbits. The 9:4 is globally chaotic, with a time scale to reach a planet-crossing orbit being ~50 My (6). The complex 2:1 has active portions at small e or large librational amplitudes where escape is possible on ~10-My time scales; the central region is only active on 0.1-billion- to 1-billion-year time scales (22), producing the large fraction of surviving particles (Table 1).

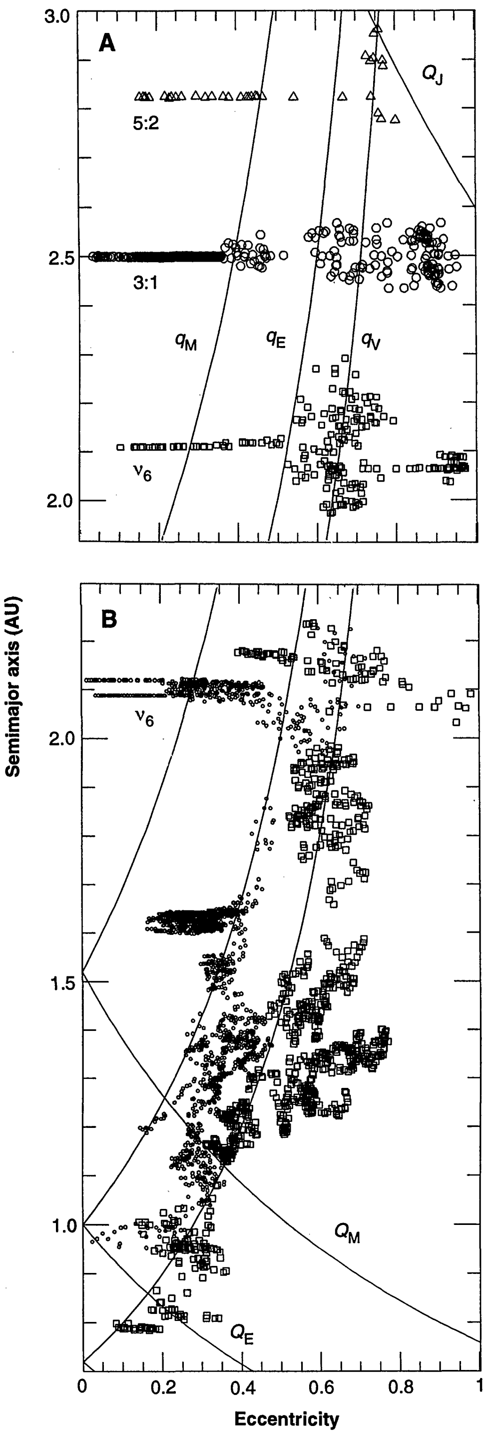

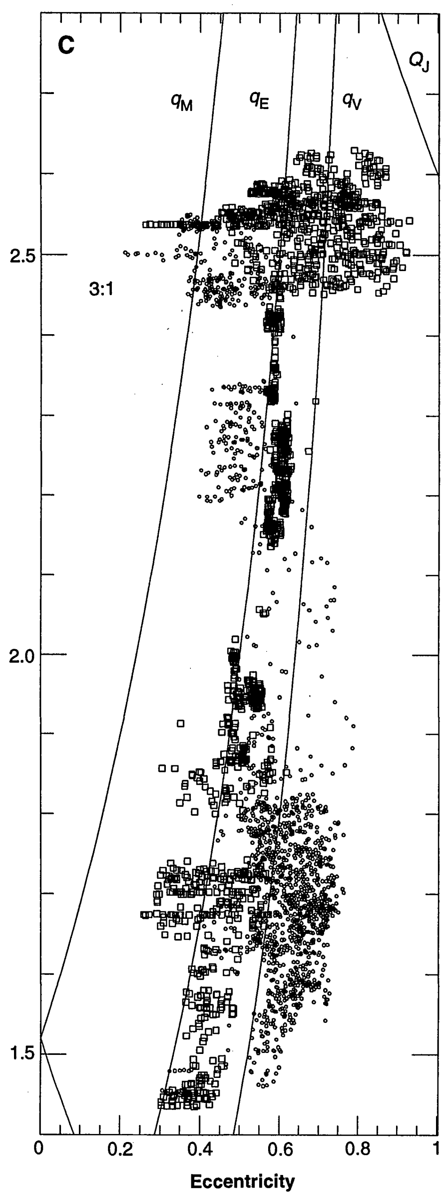

Fig. 3. Orbital evolutions of objects leaving the main belt. The curves indicate the set of orbits having aphelion (Q) or perihelion (q) at the semimajor axis of one of the planets Venus, Earth, Mars, or Jupiter. (**A**) Common evolutionary paths from three resonances. An object (triangles) from the 5:2 is extracted by Earth or Venus and is pushed to cross the orbit of Jupiter (curve at upper right) and quickly removed from the inner solar system, requiring 0.3 My. An object (circles) from the 3:1 is pushed into the sun ($e \rightarrow 1$) without leaving the mean-motion resonance (which is considerably wider at large e), taking 5 My. An object (squares) from the ν_6 is temporarily extracted by Earth or Venus before reentering the resonance (at a different inclination and thus different a) and becoming a sun-grazer after 2 My. (**B**) A long-living particle from the ν_6. Points are dots before 20 My and squares after. (**C**) A long-living particle from the 3:1 shows many episodes of horizontal (resonant) oscillations. Points are dots before 15 My and squares after.

Our integrations indicate that Jacobi constants (23) are poorly conserved on million-year time scales as objects migrate toward smaller a; the particles simply transit too many resonances that are capable of modifying their orbits, and as particles migrate to smaller a their perihelion distances undergo large variation (Fig. 3, B and C). We also observed the production of highly inclined NEA orbits. Of particles that spend more than 1 My with $a < 2$ AU, one-third exceed $i = 25°$ at some time as a result of the action of the ν_{13}, ν_{14}, or ν_{16} secular resonances or close encounters; for example, the object of Fig. 3C is raised from $i = 20°$ to 40° by ν_{16} when $a \simeq 1.7$ AU. These processes are probably sufficient to explain the highly inclined component of the NEA population (20, 24).

The literature discusses two "martian slow tracks" that might allow objects to reach Earth $\geq 10^8$ years after their resonant emplacement event. In the first, particles extracted by Mars subsequently evolve through repeated encounters with Mars, following curves of quasi-constant Jacobi constant in $\sim 10^8$ years to Earth-crossing orbits [see figure A2 in (14)]. Our simulations provide no evidence for the existence of this slow track. For the 3:1 and ν_6, only about 5% of the particles are extracted by Mars before Earth-crossing is achieved. The majority of these are pushed back into the resonance by a subsequent encounter. The median time spent extracted is 14 My for the 3:1 and 6 My for the ν_6. No particle was ever seen to migrate below $a = 1.8$ AU while in the solely Mars-crossing region; even if it did, other resonances like the 4:1 or the second-order secular resonances near 1.7 AU (19) would arrest its migration. Mars encounters are simply too weak to permit particles to jump over resonances and prevent pumping to Earth-crossing orbits; therefore, this first mechanism exists for $\ll 1\%$ of the injected particles and is not a dynamically important phenomenon. A second martian slow track, in which particles reach Mars-crossing orbits only near the top of their eccentricity cycle near the border of the ν_6 resonance and enter deeper in the resonance only on a long time scale (*15, 25*) as a result of martian close encounters, is not well explored by this set of initial conditions. Additional integrations of this phenomenon confirm its existence for a small fraction of the resonant phase space ($\approx$0.05 AU); deep Mars-crossers ($q < q_{Mars}$) rarely survive for >10 My, and only shallow Mars-crossers ($q_{Mars} < q < Q_{Mars}$) can remain in this state for tens of millions of years.

Implications

If the NEA population is in steady state, our new shorter dynamical lifetimes imply a correspondingly larger injection rate. On the other hand, to produce tens of large NEAs (>5 km in diameter) presumably requires family break-up events, which are energetic enough to eject these large fragments with velocities (100 m/s) sufficient to reach the resonances (*26*). Less energetic events involving smaller bodies are not expected to produce large numbers of high-speed fragments. However, the integrations show that few fragments survive for long, which would seem to imply that the family-creation events occurred more recently (100 My ago) than is generally accepted (*27*). Asserting the current large NEAs to be the few survivors from the original event is unsatisfactory because the implied number of original injections is too large; for example, from the 3:1 or ν_6 resonances the particles remaining after 30 My are outnumbered by the original injections by a factor of more than 30 (*9*). A possible hypothesis is that diffusion along the resonance border allows particles to gradually "leak in"; this has been shown to occur in the Edgeworth-Kuiper Belt (*10, 28*). Perhaps higher order resonances (like the 8:3 or 9:4), which produce Earth-crossing on much longer time scales, are responsible for delivering the majority of the large NEAs that have reached Earth-crossing orbits in the last 10 My. Although particles are inefficiently extracted and stored in solely Mars-crossing orbits once they exit the main belt, asteroids could be collisionally or dynamically emplaced in slightly Mars-crossing orbits far from resonance, where they could survive for a long time before being pushed by Mars into resonance. Lastly, some fraction of the NEAs may be devolatilized comet nuclei rather than asteroids (*24*).

Meteoroids only begin accumulating cosmic-ray exposure (CRE) after being liberated (*29*) as bodies <3 m in diameter or while resting within ~1 m of a larger body's surface. If chondrites resulted from a continuous supply of meteoroids launched from shielded locations directly into the 3:1 resonance, our simulations indicate that the majority of them would have CRE ages of <5 My—in contrast to the CRE data (*30*). Thus, the liberation event cannot also have placed the meteoroids in the resonance. Particles from ν_6 can arrive on a more satisfactory time scale, but most Earth impacts come from highly evolved orbits (*9*) and cannot by themselves satisfy known orbital constraints (*31*). Our results imply that most CRE is accumulated in bodies of ~10 to 300 cm in diameter with orbits confined inside the main belt before some subsequent process places them in resonance, after which they are delivered rapidly to Earth (*32*). If a collisional process is responsible for the final emplacement into resonance, it could result in a complex exposure history; in cases where such histories are established, they often conform to the above scenario of a long (10 to 100 My) first stage in a body of ~1 m or more and a short second stage of less than 5 My in a smaller body (*33*).

REFERENCES AND NOTES

1. See J. Wisdom, *Nature* **315**, 731 (1985); G. W. Wetherill, *Icarus* **76**, 1 (1988), and references therein.
2. See reviews by S. Ferraz-Mello, in *Asteroids, Comets, Meteors 1993*, A. Milani, M. Di Martino, A. Cellino, Eds. (Kluwer, Dordrecht, Netherlands, 1994), pp.175–188; C. Froeschlé and A. Morbidelli, *ibid.*, pp.189–204.
3. C. Froeschlé *et al.*, *Icarus* **117**, 45 (1995).
4. P. Farinella *et al.*, *Nature* **371**, 314 (1994); H. Levison and M. Duncan, *Icarus* **108**, 19 (1994).
5. An acronym for Give A Parent To Every Child. Spectral methods to establish such connections are discussed by L. A. McFadden, M. J. Gaffey, and T. B. McCord [*Science* **229**, 160 (1985)].
6. Resonance borders are the borders of the main chaotic region accounting for secular oscillations. Use of resonant proper elements allows direct determination of whether a particle is "in" the resonance or not [A. Morbidelli *et al.*, *Icarus* **118**, 132 (1995)].
7. We have used the techniques of V. Zappalà *et al.* [*ibid.* **124**, 156 (1996)].
8. A. Milani and P. Farinella, *ibid.* **115**, 209 (1995).
9. F. Migliorini *et al.*, *Meteoritics Plan. Sci.*, in press.
10. A. Morbidelli, *Icarus* **127**, 1 (1997).
11. End states, the decay of the number of particles, and the distribution of orbital elements are statistically identical over the time scale of $\approx$3 My, which is numerically feasible with conventional Bulirsch-Stoer and RADAU algorithms. See also (*9*). The symplectic algorithm is that of J. Wisdom and M. Holman [*Astron. J.* **102**, 1528 (1991)], as modified by H. Levison and M. Duncan [*Icarus* **108**, 18 (1994)]. The output (only) was numerically averaged to produce proper elements free of short-period oscillations.
12. Our results show that we accurately located resonance borders. There were usually $\approx$150 active particles (Table 1), the number we tried to place in the active zone. Exceptions were the ν_6 (all 110 particles were active), Vesta 3:1 (resonance boundaries were not used in calculating the initial conditions), and Koronis (small proper e's caused poor theoretical prediction of the resonance borders).
13. A. Morbidelli and M. Moons, *Icarus* **115**, 60 (1995); M. Moons and A. Morbidelli, *ibid.* **114**, 35 (1995).
14. R. Greenberg and M. Nolan, in *Asteroids II*, R. Binzel, T. Gehrels, M. S. Matthews, Eds. (Univ. of Arizona Press, Tucson, 1989), pp. 778–804; R. Greenberg and M. Nolan, in *Resources of Near-Earth Space*, J. Lewis *et al.*, Eds. (Univ. of Arizona Press, Tucson, 1993), pp. 473–492; W. F. Bottke *et al.*, *Icarus* **122**, 406 (1996), especially figure A2.
15. D. Rabinowitz, *Icarus* **127**, 33 (1997).
16. When objects in mean-motion resonances arrive at conjunction with that planet, they are far from the planet and thus protected from close encounters.
17. By definition, Apollo asteroids have pericenters $q <$ 1.017 AU and $a > 1$, Amors satisfy $q <$ 1.3 AU, and Atens $a < 1$ with $Q > 0.983$ [G. Shoemaker *et al.*, in *Asteroids*, T. Gehrels, Ed. (Univ. of Arizona Press, Tucson, 1979), pp. 253–282].
18. SEAs are small Earth-approaching asteroids with orbits similar to that of Earth. See (*15*).
19. B. J. Gladman *et al.*, *Science* **271**, 1387 (1996).
20. P. Michel and C. Froeschlé, *Icarus*, in press.
21. A. Milani and Z. Knežević [*ibid.* **98**, 211 (1992)] mapped this resonance near this region. Of the 165 particles, 91 begin in the 8:3 resonance (72 die), 65 begin outside the 8:3 but in the $g = 2g_6 - g_5$ resonance (10 die), and 9 begin outside both (1 dies) over the 43-My integration.
22. A. Morbidelli, *Astron. J.* **111**, 2453 (1996).
23. The Jacobi constant is a conserved quantity for the massless particle in the circular restricted three-body problem. Particles dominated by close encounters with a single planet on a circular orbit conserve their encounter velocity with respect to that planet, which results in motion in *a*-*e* space roughly parallel to lines of constant *q* (*14*). On million-year time scales, the noncircularity of planetary orbits and distant perturbations induce considerable drift in the values of the Jacobi "constants."
24. G. W. Wetherill, *Icarus* **76**, 1 (1988).
25. J. T. Wasson, *Science* **249**, 900 (1990).
26. M. Menichella, P. Paolicchi, P. Farinella, *Earth Moon Planets* **72**, 133 (1996).
27. P. Farinella, D. R. Davis, F. Marzari, in *Completing the Inventory of the Solar System*, T. W. Rettig and J. M. Hahn, Eds. (Astronomical Society of the Pacific, San Francisco, 1996), pp. 45–55.
28. M. Duncan *et al.*, *Astron. J.* **110**, 3073 (1995).
29. For stony objects, Wetherill (*24*) proposes a collisional half-life of order $\sqrt{r}$ My while in the main belt, where *r* is the meteoroid radius in centimeters.
30. K. Marti and T. Graf, *Annu. Rev. Earth Planet. Sci.* **20**, 221 (1992).
31. These constraints are established by the a.m./p.m. asymmetry in fall times and from orbits determined by fireball observations [see (*14*) and G. Wetherill, *Meteoritics* **20**, 1 (1985)]. These constraints also rule out deriving the bulk of the chondrites by breaking up asteroids already on NEA orbits.
32. The subsequent transport into resonance might be accomplished by collisional effects, slow-track motion in the ν_6, or due to the recently reconsidered Yarkovsky effect [J. A. Burns *et al.*, *Icarus* **40**, 1 (1979); D. Rubincam, *J. Geophys. Res.* **100**, 1585 (1995)].
33. S. K. Vogt *et al.*, *Meteoritics* **28**, 71 (1993); G. Heusser *et al.*, *Meteoritics Planet. Sci.* **31**, 657 (1996); R. Wieler *et al.*, *ibid.*, p. 265.
34. The distribution of asteroids relative to the gaps is pictured in S. Dermott and C. Murray, *Nature* **301**, 201 (1983).

35. We thank B. Bottke, C. Chapman, O. Eugster, P. Farinella, K. Marti, and G. Wetherill for constructive input to this study. T. Bowell provided the initial conditions for the NEA sample.